AIP | The Journal of Chemical Physics

Intermolecular modulation of IR intensities in the solid state. The role of weak interactions in polyethylene crystal: A computational DFT study

Daria Galimberti, Alberto Milani, Lorenzo Maschio, and Chiara Castiglioni

Citation: The Journal of Chemical Physics **145**, 144901 (2016); doi: 10.1063/1.4964500
View online: http://dx.doi.org/10.1063/1.4964500
View Table of Contents: http://scitation.aip.org/content/aip/journal/jcp/145/14?ver=pdfcov
Published by the AIP Publishing

Intermolecular modulation of IR intensities in the solid state. The role of weak interactions in polyethylene crystal: A computational DFT study

Daria Galimberti,[1,2] Alberto Milani,[2] Lorenzo Maschio,[3] and Chiara Castiglioni[2,a)]
[1]*LAMBE CNRS UMR8587, Laboratoire Analyse et Modélisation pour la Biologie et l'Environnement, Université d'Evry val d'Essonne, Boulevard F. Mitterrand, Bat Maupertuis, 91025 Evry, France*
[2]*Dipartimento di Chimica, Materiali e Ingegneria Chimica Giulio Natta, Politecnico di Milano, Piazza Leonardo da Vinci 32, 20133 Milano, Italy*
[3]*Dipartimento di Chimica, Università di Torino and NIS (Nanostructured Interfaces and Surfaces) Centre, Via P. Giuria 5, 10125 Torino, Italy*

(Received 20 June 2016; accepted 27 September 2016; published online 14 October 2016)

Density functional theory calculations with periodic boundary conditions are exploited to study the infrared spectrum of crystalline polyethylene. Spectral changes lead by the intermolecular packing in the orthorhombic three-dimensional crystal are discussed by means of a careful comparison with calculations carried out for an isolated polymer chain in the all-trans conformation, described as an ideal one-dimensional crystal. The results are analyzed in the framework of the "oligomer approach" through the modelling of the IR spectrum of n-alkanes of different lengths. The study demonstrates that a relevant absorption intensity modulation of CH_2 deformation transitions takes place in the solid state. This finding suggests a new interpretation for the experimental evidences collected in the past by means of IR intensity measurement during thermal treatment. Moreover, the comparison between calculations for 3-D crystal and for the isolated polyethylene chain (1-D crystal) allows to put in evidence the effect of the local electric field on the computed infrared intensities. This observation provides guidelines for the comparison between infrared absorption intensities predicted for an isolated unit and for a molecule belonging to a crystal, through the introduction of suitable correction factors based on the refraction index of the material and depending on the dimensionality of such units (0D—molecule; 1D—polymer; 2D—slab). *Published by AIP Publishing.* [http://dx.doi.org/10.1063/1.4964500]

I. INTRODUCTION

The study of intermolecular interactions and their role in determining the supra-molecular architecture is an evergreen topic in materials science. However, because of their intrinsic nature, the careful theoretical description of such interactions is a difficult task, since weak dispersion forces often require non-trivial modelling in the framework of a quantum chemical approach.

On the other hand, experimental data affected by the interactions occurring in the condensed phases offer unique opportunities for the understanding of the underlying physical phenomena and for the validation of the theoretical models.

The spectroscopic response in the IR is often a sensitive probe of intermolecular interactions and experimental markers related to the presence of specific interactions can be and have been exploited for the recognition and for the characterization of supra-molecular structures.[1,2] In this framework, it is well known that strong intermolecular interactions such as hydrogen bonds[3] determine huge changes of the IR spectral pattern (shift of peaks frequencies, often accompanied by dramatic changes of the intrinsic absorption intensities). In presence of H bonds, the analysis of the spectral features provides very effective tools for the structural diagnosis, especially when the experimental data are analyzed in conjunction with quantum chemical modelling.[4–9] Also, the structure of crystalline phases can be investigated by means of IR spectroscopy (see, for instance, Refs. 4, 6, and 10–17, and bibliography herein). In this case, symmetry selection rules determined by the crystal structure play a key role in the proper bands assignment and often allow to discriminate among different models of the crystal unit cell. Investigations on crystalline polymorphs, especially the field of polymer science, are based on the careful assignment of IR features.[4,6,10–17]

A comprehensive interpretation of the vibrational spectra of semi-crystalline polymers is a very intriguing and non-trivial topic, because in this case several different concurrent structural effects determine the spectral pattern of the material:

(i) The conformation of the polymer chains belonging to a crystal must fulfil the requirement of ***regularity***. In other words, the structure of the chain is described as a repetition along the chain axis of small translational units linked by covalent bonds. Accordingly, the single polymer chain can be modelled as an ideal 1D crystal;
(ii) Polymer chains are packed in a 3D crystal structure, characterized by a suitable crystal cell.
(iii) According to the space group symmetry of the crystal, IR selection rules for the optical phonons at the Γ point

a)Author to whom correspondence should be addressed. Electronic mail: chiara.castiglioni@polimi.it

of the first Brillouin zone rule the occurrence of IR transitions.

(iv) The unavoidable presence of the amorphous phase contributes to the IR spectrum with broad features, often superimposed to the sharp absorptions of the crystalline material; sometimes it gives rise to some specific "defect" bands.

While interpreting the IR spectrum of a semicrystalline polymer, it is mandatory to recognize in a unambiguous way the consequences of points i-iv and to clearly disentangle the different effects. On this basis, markers related to the occurrence of a regular conformation of the chains (i.e., "regularity" bands), as well as features associated to intermolecular interactions responsible of the crystal packing (i.e., "crystallinity" bands) could be identified.[4,10–15,18]

In the past, this kind of analysis was mainly based on several systematic and sophisticated experimental studies, including the analysis of thermal evolution of the spectra and a careful comparison with spectra of oligomers with known structure (see, for instance, Refs. 19–21 for the case of polyethylene and n-alkanes). Bands assignment was led by the predictions of phonon frequencies based on empirical harmonic force fields, in the framework of space group symmetry theory. The so called "oligomer approach"[10–15] allowed to increase the set of experimental data in order to develop empirical correlations based on the direct comparison of the spectra. In this framework, the availability of peaks frequencies of oligomers was of fundamental importance for the development of reliable empirical vibrational force fields by means of overlay procedures. Also defect modes ascribed to amorphous phases or structural defects inside the crystals were modelled considering vibrational dynamics of short molecules (oligomers) in different conformations.

Several papers and reviews dealing with IR spectroscopy applied to semicrystalline polymers have appeared between 1960 and 1980 (for a complete bibliography see, for instance, Refs. 10–15) and are still considered the reference for the rationalization of the vibrational behaviour of such materials. In this framework, the analysis of the IR spectrum of polyethylene (PE) and related oligomers (linear n-alkanes) should be certainly considered a milestone and a paradigm.

Today, thanks to the growth of the computational capabilities and to the development of powerful quantum chemical models, algorithms, and software codes, the analysis of the IR spectra can be made more and more effective by adopting suitable *first principles* theoretical modelling. In particular, the implementation of the translational symmetry in quantum chemical codes exploiting the MO = LCAO methods and the use of the full space group symmetry, allowed to extend the simulation of IR and Raman spectra to rather complex molecular crystals and in particular to polymer crystals. CRYSTAL[22,23] code has proven to be very effective for these studies.[4,5,17,18,24–28]

Unlike the previous empirical works, which were mainly restricted to the prediction of vibrational frequencies, first principles calculations provide IR absorption intensities and Raman activities, which in turns allow a direct comparison with the experimental intensity pattern. Notice that absolute intensity values, which are hardly available through solid state experiments, can be theoretically predicted.

The possibility to compute reliable vibrational spectra in solid phase paves the way to a further validation of the already established correlations between spectral features and polymer structure and can help in disentangling subtle intra-molecular and inter-molecular effects which still remained obscure. Moreover, it provides tools for a deeper rationalization of these effects. In particular, while the effect of intermolecular interactions on frequencies, as for instance, the occurrence *crystal splitting* of bands, has been interpreted since long time in the framework of classical vibrational dynamics, the consequence of crystal packing on absorption intensities remained so far a rather elusive matter, because of difficulties associated to absolute intensities measurement and to the intrinsic limitation of the classical approaches for the modelling of absorption intensities.

In this paper, we will revisit the well-established case of the IR spectrum of PE, by means of Density Functional Theory (DFT) calculations with periodic boundary conditions (PBC), applied to the modelling of the structure and of the IR spectrum of its orthorhombic crystalline phase. The study is aimed at exploring potentialities and limitations of this approach, focusing in particular on the effects of the crystal field on IR intensities and on the performances of the CRYSTAL code[22,23] in this respect.

II. THE IR SPECTRUM OF POLYETHYLENE: A SHORT REVIEW

The IR spectrum of highly crystalline polyethylene samples (see Figure 1) has been experimentally investigated and rationalized in the framework of the classical vibrational dynamics by several authors.[29–33] More recently, theoretical studies on PE and its oligomers, based on quantum chemical modelling, appeared in the literature.[34–36]

On these grounds, the assignment of the spectral features can be considered a well-established matter.

The vibrational assignment of the IR transitions can be made firstly considering IR active phonons of a single, infinite chain in the all-trans conformation—one-dimensional (1D) crystal—which line group is isomorphous to the D_{2h} symmetry point group, at Γ point.

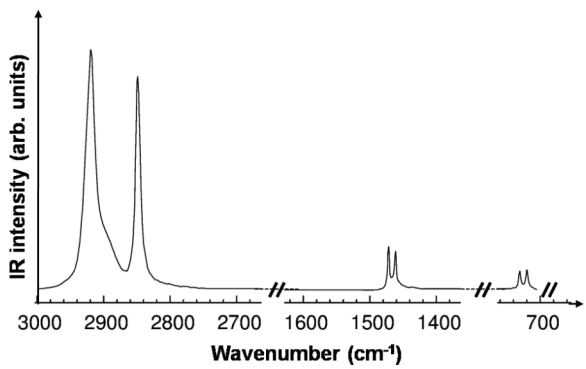

FIG. 1. IR spectrum of a highly crystalline PE sample (adapted from Ref. 32).

Accordingly, IR active phonons are classified and described as combination of symmetry adapted internal coordinates of the chemical unit (CH_2), as reported in Table I. Due to the high symmetry and to the very small mixing between the high energy CH stretching vibrations with bending vibrations of PE, the IR transitions are usually described as "pure" d−, d+, δ, W, P, namely, anti-symmetric and symmetric CH_2 stretching, CH_2 scissoring, wagging, and rocking (the experimental frequencies are reported in Table I). In other words, one assumes that the phonon can be identified with the symmetry coordinate with the major contribution in the vibrational eigenvector (see Ref. 33 for the definition of symmetry coordinates and for a detailed discussion).

The crystal packing in the three-dimensional (3D) crystal, described by the orthorhombic cell with two chains per unit cell, determines the doubling of the IR active phonons of B_{2u} and B_{3u} species, and the symmetry coordinates of the crystal are usually described as the in phase and out-of-phase combinations of the coordinates defined for the 1D crystal—see Table I.

While in the stretching region the effect of the crystal packing cannot be easily recognized because of the small crystal splitting and to the complex band structure (ascribed to the occurrence of Fermi resonances[37,38]), bending and rocking peaks show indeed the characteristic splitting into two IR active components, of comparable intensity.

This peculiar behavior has been taken as the signature of the orthorhombic cell, containing two different PE chains. It perfectly parallels the IR features observed for crystalline sample of odd-numbered crystalline n-alkanes, which indeed are packed according to an orthorhombic structure with two dynamically coupled chains. On the opposite, the crystal splitting is lost in the case of even-numbered n-alkanes crystal both packed according to the monoclinic cell (because of different symmetry selection rules) or triclinic cell with one molecule per unit cell.[39] Crystal splitting shown by the orthorhombic crystals is sensitive to thermal expansion and disappears during the pre-melting phase characterized by expansion of the crystal cell and activation of collective large amplitude torsional motions of the chains.[10–15,40] Crystal splitting of rocking and scissoring bands of PE has been discussed thoroughly and models describing the vibrational coupling between neighboring chains by means of the introduction of inter-molecular force constants have been proposed.[39]

The intensity pattern of the IR spectrum of PE can be qualitatively described as follows: The CH stretching bands dominate the whole spectrum, showing absorbance values about ten times larger than the deformation bands (in the following the sum of the integrated absorption intensities of scissoring and rocking bands will be simply referred as "deformation" intensity). Even if a wagging transition is expected to occur in the IR on the basis of symmetry, its activity is so weak that it cannot be recognized in the experimental spectrum. The spectral region between 1400 cm^{-1} and 1300 cm^{-1}, which is free from fundamental transitions of the crystalline phase, can show peculiar wagging marker bands ascribed to the occurrence of conformational defects, which can be characterized and quantified on this basis.[10–14,40] A rationalization of the intensity behavior of the wagging band which is silent in *trans*-planar polymethylene chains and shows-up in the presence of gauche defects is reported in Ref. 41.

Absorption intensities of PE have been deeply analyzed by Abbate *et al.* in Ref. 33, who reported integrated areas relative to the absorption bands associated to the fundamental IR transitions for solid samples of PE and for its per-deuterated derivative, both characterized by high crystallinity. For the first time in Ref. 33, a prediction of the IR absolute intensities of PE is proposed, based on experimental intensity parameters (electro-optical parameters) obtained by means of the parameterization of absolute intensities of small oligomers in the gas phase.[42] The authors adopted a model of "isolated" PE chain (1D infinite crystal) thus neglecting intermolecular electro-optical interactions. According to the authors, this lacking can be one of the reasons for the unsatisfactory prediction of the intensity ratios between the CH stretching intensities and the deformation (rocking and scissoring) ones.

Beside the evidences of intermolecular interactions in the crystalline phase in terms of peaks frequencies (e.g., occurrence of doublets), Snyder *et al.*[43,44] showed that also IR intensities are sensitive to the phase of the sample. In Ref. 43, very accurate experimental studies on the temperature behavior of IR intensities of PE and odd-numbered alkanes ($C_{17}H_{36}$, $C_{19}H_{40}$, $C_{21}H_{44}$) are reported. As already observed by Casal *et al.*,[45] for all the samples examined, deformation intensities show a drastic drop at the solid-solid transition between the orthorhombic and the hexagonal phase; moreover a further linear intensity decrease is observed while approaching melting. A loss of about 2/3

TABLE I. Classification of the IR active phonons of PE according to the 1D crystal model (all-trans, infinite, isolated chain) and the 3D crystal model.

Symmetry coordinate mainly involved (translational unit, single chain)	Symmetry species (1D crystal, single chain)	Symmetry species (3D crystal)	Experimental frequency (cm^{-1})
d+ (out-of-phase symmetric stretching)	B_{3u}	B_{2u}, B_{3u}	2846
δ (out-of-phase scissoring)	B_{3u}	B_{2u}	1473
		B_{3u}	1463
W (in phase wagging)	B_{1u}	B_{1u}, A_u	...
d− (in phase antisymmetric stretching)	B_{2u}	B_{2u}, B_{3u}	2915
P (in phase rocking)	B_{2u}	B_{2u}	730
		B_{3u}	722

of the overall deformation intensity from the low temperature solid phase to the gas phase is reported in Ref. 43. On the opposite, CH stretching intensities seem to be weakly sensitive to temperature changes. The observed behavior of n-alkanes and PE has been confirmed by the subsequent studies.[44]

In Ref. 43, the authors discuss the possible intensity-loss mechanisms and demonstrate that neither changes of the material density, nor the refractive index variation with temperature or the occurrence of conformational disorder can quantitatively justify the observed intensity loss, which can be indeed considered as an intrinsic phenomenon. A possible interpretation has been suggested in Ref. 43 where the weakening of the deformation bands while increasing temperature is ascribed to the activation of large amplitude low frequency "lattice-like" and torsional modes, showing mechanical coupling with higher frequency normal modes.

The above interpretation was based on the idea that the intermolecular packing, determined by the weak dispersion interactions between chains, has a negligible effect on the electron density distribution and dipole derivatives. This same hypothesis is at the basis of the determination of the setting angle of PE chain in the orthorhombic cell[46] through the experimental measure of the intensity ratios of the two components of the rocking and scissoring doublet. The simple model proposed was based on the description of the dipole variation associated to the two phonons of the 3D crystal as a vector sum of the dipole derivatives of two non-interacting chains. Notice that, according to this model, the sum of the intensities of the bands which constitute a given doublet should be exactly twice the intensity of the corresponding vibrational mode of the single chain. Unfortunately, the experimental intensities of a single isolated all-trans chain cannot be obtained, because the all-trans regular structure occurs just in the crystal.

As shown in this study, the computational tools now available allow us to face the issue of the rationalization of the observed intensity trends with temperature from a completely new point of view, based on first principle prediction of the absolute IR intensities of a 1D crystal (single isolated PE chain) and of the 3D crystal. Comparison with calculations carried out on oligomers *in vacuo* and in their crystalline phase will be also presented, in order to discuss the reliability of computed absolute intensities of the polymer.

The experimental IR intensity data of PE are reported in Ref. 33 as relative values; absolute IR intensity values measured for low temperature samples—cooled in liquid nitrogen—are available only for short (from C4 to C8) crystalline n-alkanes.[47]

Even if a quantitative comparison between absorption intensities of PE and short n-alkanes cannot be made because of the contribution of methyl groups in oligomers, we can observe that, similarly to PE, n-alkanes intensity values in the deformation region are about one order of magnitude weaker than absorptions of the stretching bands.

III. COMPUTATIONAL DETAILS

For geometry optimization and IR spectra predictions, we adopted in this work two different protocols of simulation:

- PBC-DFT simulations have been carried out by means of CRYSTAL14 code,[22,23] to model crystals of PE (1D crystal, namely, the isolated chain with PBC in the only chain axis direction and 3D crystal) and hexane.
- DFT calculations by means of Gaussian09 code,[48] to model several n-alkanes. Both molecules *in vacuo* and small clusters have been considered.

In all the cases, the geometry optimization and the prediction of the IR spectra have been carried out adopting the B3LYP[49,50] hybrid exchange-correlation functional together with the 6-31G(d,p) basis set. For modelling the crystals and clusters, the B3LYP functional has been augmented with an empirical correction for dispersion interaction (B3LYP-D2) proposed by Grimme[51–53] and implemented both in CRYSTAL14 and Gaussian09.

Gaussian09 program adopts the sets of parameters proposed by Grimme[51,52] for the description of the dispersion correction, while in the case of calculations carried out with CRYSTAL code, we adopted the sets of parameters proposed by Quarti *et al.*[4] These parameters have shown indeed to give the best performance for several polymers.[6,16,18]

In PBC calculations, full geometry optimization (cell parameters and atomic positions) of the structure of

- the isolated infinite PE chain in its regular all-trans conformation,
- finite clusters of infinite PE chains, and
- the orthorhombic PE crystal

have been carried out by means of the CRYSTAL14 code.[22,23] The IR intensities have been predicted according to the coupled-perturbed Hartree–Fock/Kohn–Sham approach, as implemented in the code.[54]

In the case of the calculations on PE crystal while increasing the cell parameters (expanded cell) reported in Section IV B, cell parameters have been fixed and the atomic positions only have been optimized. As starting guess structures for the calculations, we considered the experimentally determined crystal parameters and atomic coordinates reported by Bunn *et al.*[55]

In all the cases considered, the vibrational spectrum has been predicted in double harmonic approximation for the equilibrium structures, through the calculation of second derivatives of the potential energy (frequencies) and first derivative of the dipole moment (IR intensities).

In some cases (e.g., clusters and short alkanes), we modified the masses of given groups of atoms with a fictitious value of 5000 amu, in order to remove the contribution to the spectrum of the CH_3 groups or of the chains in the external shells.

Different functional/basis set combinations have been tested (with and without the Grimme correction for the interactions) and compared. For sake of conciseness, in the following discussion we will focus mainly on the results obtained with B3LYP/6-31G(d,p) calculations. This choice follows from previous studies on the modeling of crystalline polymers often characterized by the occurrence of different polymorphs.[6,16,18] These studies showed the

good performances of this computational setup both for the prediction of crystal structures and of the vibrational spectra.

It is however important to stress that despite a certain sensitivity of the results from the adopted functional—that we will document in Section IV—the main conclusions drawn in this study have a general character.

IV. RESULTS AND DISCUSSION

A. 3D crystal vs 1D chain

Using the program CRYSTAL14 and applying PBC, we predicted the IR spectrum for both the whole crystal (according to the observed 3D crystalline structure) and an isolated infinite 1D chain characterized by a perfect *trans*-planar conformation.

In Figure 2, we report the plot of the computed spectrum for 3D and 1D crystals. In the plot, the computed intensities of each transition are normalized to the number of CH bonds in the unit cell.

The comparison of the theoretical spectrum obtained for the 3D crystal with the experimental one (Figure 1, Table II) shows that the theoretical prediction accurately describes several relevant experimental features:

(i) The general intensity pattern is qualitatively reproduced. Indeed, the calculated intensity ratio between stretching and deformation region is overestimated by 35%, while the intensity ratio between scissoring and rocking bands is underestimated by 55%.
(ii) The theoretically predicted wagging band is very weak, as suggested by the experiment.
(iii) The observed crystal splitting of the scissoring and rocking bands is nicely described, even if slightly overestimated by the calculation in the case of the scissoring doublet (compare the experimental splitting values of 10 cm^{-1} and 12 cm^{-1}[46] with the predicted values of 20 cm^{-1} and 12 cm^{-1} for the scissoring and rocking bands, respectively). The predicted crystal splitting become 7 cm^{-1} for the scissoring and 2 cm^{-1} for the rocking doublet if the calculation is carried out in absence of the Grimme correction (see Table III and Figure S1 in the supplementary material), confirming that this correction is mandatory to obtain an optimized geometry suitable for a reasonable prediction of the spectral features.
(iv) According to the calculations, also the CH stretching bands split, but the predicted splitting is very small (4 cm^{-1} for the d− band and 5 cm^{-1} for d+), thus justifying the fact that it has not been revealed experimentally.

TABLE II. Values of IR absorption intensities of PE 3D crystal (B3LYP-D2/6-31G(d,p) calculation) and 1D crystal (B3LYP-D2/6-31G(d,p) calculation), normalized to the number of CH oscillators.

	$I^{stretching}$/CH (km/mol)	$I^{deformation}$/CH (km/mol)	$R = I^{stretching}/I^{deformation}$	$r = I^{scissoring}/I^{rocking}$
3D crystal	75	5.26	14.4	1.02
1D crystal	31.99	0.58	55.4	0.49
Experimental[33]	...	...	9.3	2.25

The 1D model obviously does not describe any crystal splitting; moreover, it is immediately clear that the two models provide a very different picture also from the point of view of the intensity pattern (Table II):

(i) Normalized stretching intensities and deformation intensities decrease while passing from the 3D to the 1D model; moreover, the intensity ratio R between stretching and deformation intensities increases by a factor of about 4 from 3D to 1D model, showing that the intensity weakening of the deformation transitions is more drastic than for stretching transitions. Notice moreover that the experimental value of R = 9.3 is fairly well reproduced by the calculation on 3D crystal (R = 14.4), but it is dramatically overestimated by the calculation for the isolated chain (R = 55.4). Indeed, the overall IR intensity

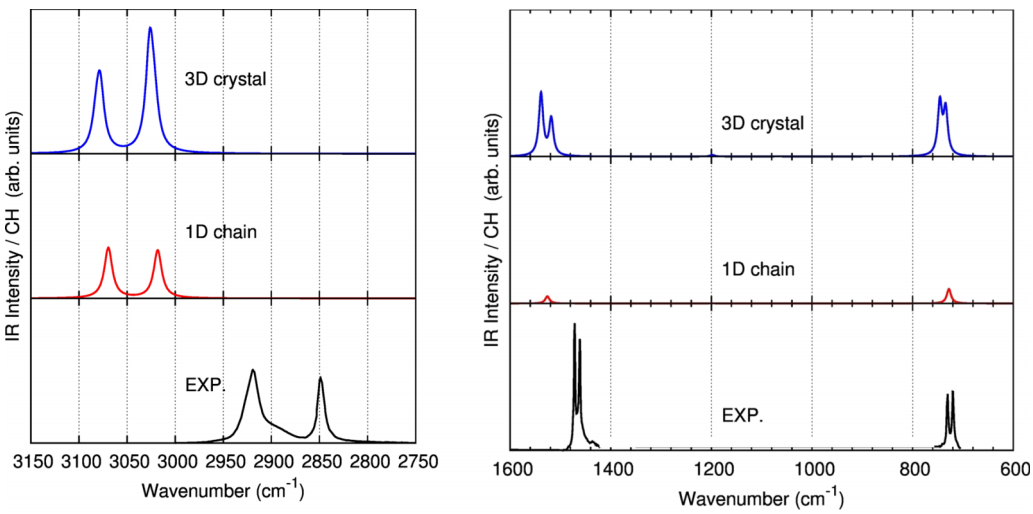

FIG. 2. Plot of the computed IR spectrum of PE 3D crystal (B3LYP-D2/6-31G(d,p) calculation) and 1D crystal (B3LYP-D2/6-31G(d,p) calculation); values of IR absorption intensities, normalized to the number of CH oscillators, are reported in Table II.

TABLE III. Predicted IR absorption intensities of PE 3D crystal (intensities are normalized to the number of CH oscillators in the unit cell), intensity ratios, crystal splitting of scissoring and rocking doublets, and crystal cell parameters obtained after optimization. Results obtained by means of different computational methods are compared in the table. In the case of B3LYP/6-31G(d,p) and in the case of HSE/6-31G(d,p), the effect of the inclusion of Grimme correction is shown.

	$I^{stretch}$/CH (km/mol)	I^{def}/CH (km/mol)	R $= I^{stretch}/I^{def}$	r $= I^{sciss}/I^{rock}$	$\Delta\nu_{sciss}$ (cm^{-1})	$\Delta\nu_{rock}$ (cm^{-1})	a (A)	b (A)	c (A)
Experimental values	...	...	9.3 (Ref. 33)	2.25 (Ref. 33)	10	12	4.93, 4.85 (Ref. 56)	7.40, 7.12 (Ref. 56)	2.534, 2.548 (Ref. 56)
B3LYP/6-31G(d,p)	63.98	1.41	45.45	0.35	7.18	2.36	5.50	9.27	2.57
B3LYP-D2/6-31G(d,p)[a]	75.74	5.26	14.39	1.02	20.35	11.43	4.85	7.05	2.57
B3LYP-D2/6-31G(d,p)[52 b]	64.64	7.72	8.38	1.00	8.36	27.9	4.45	6.48	2.55
B3LYP-D3/6-31G(d,p)[52 c]	74.28	5.96	12.47	1.13	14.65	16.40	4.76	6.88	2.56
B3LYP-D2/pob-TZVP[a]	73.97	5.30	13.96	0.87	24.35	18.95	4.68	7.06	2.55
PBE0-D2/6-31G(d,p)[b]	67.48	8.02	8.41	1.18	25.4	20.11	4.73	6.93	2.55
BLYP-D2/6-31G(d,p)[a]	81.15	4.56	17.18	0.73	7.75	17.45	4.91	7.14	2.59
PBE-D2/6-31G(d,p)[a]	71.31	7.35	9.70	0.90	24.5	15.28	4.75	7.00	2.57
PBE-D2/TZVP[a]	66.03	8.32	7.93	1.40	25.28	12.97	4.77	7.01	2.56
PBE-D3/6-31G(d,p)[51,52 c]	72.30	7.22	10.01	0.91	16.68	12.04	4.85	7.05	2.57
LC-BLYP/6-31G(d,p)	58.09	7.77	7.47	1.50	14.79	9.78	4.83	7.04	2.54
HSE/6-31G(d,p)	65.08	4.38	14.86	0.97	10.71	4.69	5.34	7.87	2.55
HSE-D3/6-31G(d,p)[51,52 c]	67.29	7.10	9.47	1.18	16.45	13.12	4.82	7.04	2.55

[a]Grimme parameters from Ref. 4
[b]Standard Grimme parameters from Ref. 52
[c]Standard Grimme parameters from Refs. 51, 52

predicted for the region of the deformation vibrations is 10 times smaller for the single chain compared to the 3D crystal.

(ii) The comparison between the two theoretical models indicates that the CH stretching bands in the 3D crystal are blue shifted by the crystal field. The predicted shifts are 10 cm^{-1} for d− and 5 cm^{-1} for d+ bands; this finding parallels the optimized values of CH equilibrium bond length, which are also slightly affected by the crystal field: r^0_{CH} = 1.098 A in the 3D crystal, r^0_{CH} = 1.100 A in the isolated chain. The above prediction seems to reflect a physical effect, in the light of the observation of thermally induced shift of the CH stretching features toward lower wavenumbers reported in Ref. 56 for PE.

While the spectrum predicted for the 3D crystal is acceptable if one considers the experimental intensity ratio between the CH stretching and deformation regions, it fails in the estimation of the intensity ratio of the two d+ and d− bands. In particular, the calculation overestimates the intensity of the lower frequency d+ band, a feature which could be partially ascribed to the fact that the CH stretching region is heavily affected by phenomena related to anharmonicity, which is proven for instance by the occurrence of Fermi resonances in this region. These effects are completely neglected by the calculation, which exploits a fully harmonic model of the intramolecular potential. Notice however that the CH stretching intensity pattern predicted with the 1D crystal model is very different, showing almost equal IR intensity for the d+ and d− bands.

A deeper analysis based on the comparison of computed vibrational eigenvectors shows a non-negligible mixing of the d+ and d− vibrational coordinates (symmetry coordinates of the isolated chain) in the four IR active CH stretching phonons (B_{2u} and B_{3u} symmetry) of the 3D crystal. This feature does not conflict with the 3D crystal symmetry and could justify the different intensity patterns shown by the CH stretching region of the 3D model and of the 1D isolated chain. The discrepancies found while comparing with the experimental features could indicate that the predicted mixing for the 3D crystal is overestimated.

The remarkable overall increase of the IR intensity values while increasing dimensionality (i.e., from 1D to 3D crystal) can be rationalized if one considers that dipole derivatives with respect to atomic displacements (Born Charges) are calculated for an ideally infinite 3D crystal, namely, the theoretical model describes the response of a bulk material. As opposite to the finite case, here the external field never crosses boundaries (interfaces) between regions of space with different refractive indices, and propagates inside an infinitely homogeneous dielectric medium.

A completely different situation occurs while predicting the bulk optical properties of a molecular material by means of quantities determined for an isolated molecule (*in vacuo*). This case has been faced in the past and explicit introduction of local field factors has been suggested in order to obtain the relationships between molecular polarizabilities and hyperpolarizabilities (computed *in vacuo*) and bulk susceptibilities.[57,58]

In systems with reduced dimensionalities (slabs, polymers, molecules), the field inside the system is smaller than the external field, due to the induced internal field, hence the polarization response is also smaller. The relationship with polarization in the 3D bulk depends on the geometry of the system[54,59,60] so that a conversion factor (F) linking Born charges can be obtained as follows:

- For a 2D periodic slab polarized in the direction perpendicular to the slab the model is that of a condenser, then $F = \varepsilon$.
- A 1D periodic polymer can be inscribed inside an infinite cylinder, and $F = (\varepsilon + 1)/2$ (polarization perpendicular to the cylinder axis).
- A molecule ("periodic" in 0 dimensions) can be inscribed inside a sphere, and the local field correction factor is the well-known Lorentz factor $F = (\varepsilon + 2)/3$.

The second case listed above is the one relevant to the present discussion, where the dielectric tensor components along the directions orthogonal to the polymer chain are nearly identical and equal to $\varepsilon = 2.3$. As a consequence, the correction factor linking intensities for the isolated chain and in the bulk is predicted as $F^2 = 2.72$. This factor applies to the intensities of all vibrations uniformly—considering that in PE chain stretching and bending (scissoring and rocking) vibrations are polarized orthogonal to the polymer chain.

Such correction factor can be used to predict absolute vibrational intensities in the bulk, once known the result for the isolated unit, in the hypothesis of electron densities that overlap only partially. Additional effects, related to specific local interactions between the chains in the packed arrangement, usually lead to smaller effects on intensities, but can alter significantly the ratio between the peaks. These can be evaluated by constructing a sufficiently thick 1D-periodic *bundle* of PE chains (*vide infra*). In that case, it is seen that the above discussed relation for F holds exactly in this case.

Conversely, intensity changes from 1D to 3D model, which selectively affect some normal modes can be taken as the evidence of the occurrence of specific intermolecular electro-optical interactions.

In conclusion, the comparison of the computed intensity data with the experimentally available determinations suggests that the calculation on the 3D crystal of PE:

- Predicts an overall enhancement of the IR intensities of a factor larger than 2 with respect to the calculation for the single chain. This behaviour is related to the local field effects in the bulk, which are intrinsically included in the calculations for the 3D crystal.
- It nicely reproduces the intensity trend experimentally observed for the deformation intensities. Indeed, calculations indicate that the deformation intensities are remarkably more sensitive than the CH stretching ones to the 3D packing, as observed in the past by Snyder.[43,44] In his experimental work, a dramatic decrease of the scissoring and rocking intensities while approaching the pre-melting phase was indeed observed.

It is important to stress that our calculations do not take into account explicitly the effect of the temperature nor possible coupling of stretching and—thermally activated—large amplitude torsional vibrations, which is proposed in Ref. 43 as possible responsible for the intensity evolution with temperature. According to our results, we can state that the observed drastic increase of deformation intensities observed for low temperature solid phase should be mainly ascribed to the close packing of the chains, led by intermolecular interactions.

In this regard, it is interesting to analyse the effect of Grimme correction on IR intensities.

From the data reported in Table III, we can see that in absence of Grimme correction (B3LYP/6-31G(d,p)), and therefore partially neglecting intermolecular interactions, the calculation for the 3D crystal predicts an intensity ratio between stretching and deformation intensities R = 45.45, close to the one obtained for the isolated chain (R = 55.4, see Table II). Indeed the introduction of the Grimme correction—though not entering directly into the description of the wavefunction—determines an enhancement of the deformation region of factor of 4, while only slightly modifies the absorption intensity of the CH-stretching region. The remarkable modulation of deformation intensities obtained with Grimme correction can be ascribed to the concomitant shortening of the inter-chain distance, which indeed brings to a better agreement with the experimental data (compare predicted values of a and b cell parameters reported in Table III). This observation further validates the conclusion that the intensity rise of deformation bands in the 3D crystal is the indirect consequence of intermolecular interactions between adjacent chains.

In Table III, results obtained for the simulations of 3D crystal by means of several functional/basis set combinations different from B3LYP/6-31G(d,p) are reported, and in the supplementary material, the resulting theoretical spectra are compared (Figure S1). Even if the predicted values of the spectroscopic observables show a remarkable dependence on the theoretical model adopted, it is evident that, independently on the choice of the functional/basis set combination, the experimental intensity pattern is always captured: in particular, the predicted intensity ratio R between stretching and deformation intensities is close to ten in the most of the cases.

Interestingly, calculations which predict longer a, b cell parameters (e.g., B3LYP/6-31G(d,p) or BLYP-D2/6-31G(d,p)) give lower deformation intensities and higher R values, thus supporting the idea that the degree of packing of the chains determines a remarkable modulation of deformation intensities.

The LC-BLYP functional, although not including any dispersion correction, performs remarkably well in reproducing the experimental cell parameters and intensity ratios. Regarding the latter quantity, we recall that this functional was shown to outperform other functionals in describing response properties of molecules and periodic systems.[61,62]

Also in the case of HSE/6-31G(d,p) calculation, the predicted absorption intensities are quite well predicted, even without dispersion correction; however, the agreement with the experimental intensity pattern is clearly improved if Grimme correction is adopted, as a consequence of a remarkable shortening of the predicted cell parameters.

B. Effect of the crystal field

A way to prove the effect of the crystal field on absorption intensities is to follow their evolution while increasing the cell

size. We started from the optimized crystal cell and expanded it in both **a** and **b** directions, orthogonal to the chain axis. The resulting computed spectra are reported in Figure 3 (from the top to the bottom) for subsequent steps during the expansion, described by the expansion factor f. For each step, we fixed the values of the cell parameters and allow the relaxation of the atoms positions before the calculation of the IR spectrum. Figure 3 clearly shows that the spectrum of the isolated chain is progressively recovered while the cell expands. This demonstrates that several changes found while passing from the 1D crystal to the 3D crystal model are truly due to the inter-chain packing. Since the van der Waals interactions decay in a rather short range, already at the smaller expansion of the cell the crystal field effects are remarkably depressed (notice that the crystal splitting immediately disappears). Moreover also CH stretching band frequencies shift to values close to those of the 1D crystal at the lower cell expansion and the intensity ratio between antisymmetric and symmetric stretching bands quickly reaches the value of about 1, characteristic of the 1D case.

According to the results reported in Figure 3 and in Table IV, we can conclude that the two calculations (for the 3D crystal and the 1D isolated chain) are fully consistent.

TABLE IV. Values of the computed (B3LYP-D2/6-31G(d,p)) absorption intensities normalized to one CH oscillator of PE (3D crystal) while varying the cell volume (expansion factor f in both a and b directions, the factor of expansion reported refers to the equilibrium cell parameters). Computed (B3LYP-D2/6-31G(d,p)) absorption intensities of the isolated chain (1D crystal) are reported for comparison.

Model (expansion factor f)	$I^{stretching}$/CH (km/mol)	$I^{deformation}$/CH (km/mol)	$R = I^{stretching}/I^{deformation}$
3D crystal (f = 1)	75.74	5.31	14
1.1	74.88	3.26	23
1.2	65.65	1.87	35
1.3	58.57	1.17	50
1.5	46.22	1.03	45
1.8	40.91	0.82	50
2	38.98	0.76	51
3	33.88	0.65	53
4	33.57	0.61	55
1D crystal (f = +∞)	31.99	0.58	55

A closer look to the intensity data reported in Table IV provides an additional support to the interpretation presented in Section IV A. The CH stretching intensity decreases slowly from the value characteristic of the 3D crystal to that of

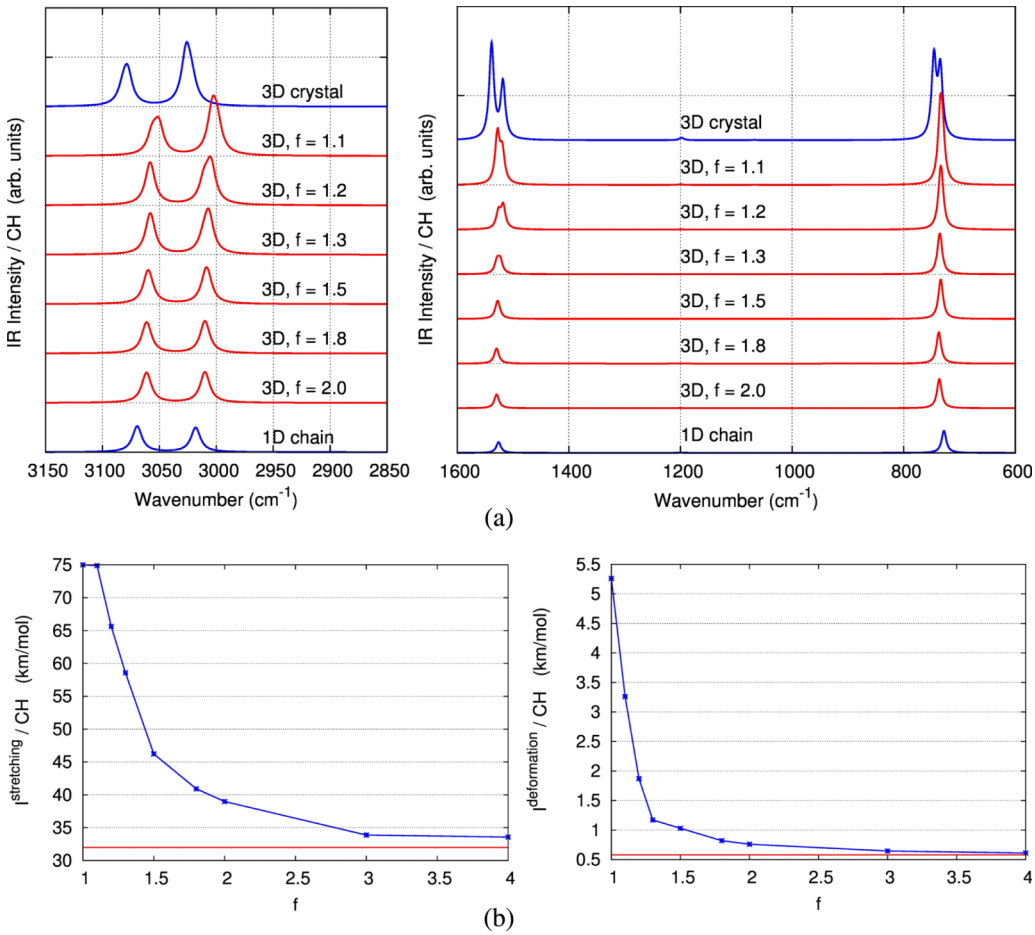

FIG. 3. (a) Plot of the computed (B3LYP-D2/6-31G(d,p)) IR spectrum of PE (3D crystal) while varying the cell volume (expansion factor f in both a and b directions), increasing from the top to the bottom (the factor of expansion reported refers to the equilibrium cell parameters), and computed (B3LYP-D2/6-31G(d,p)) IR spectrum of the isolated chain (1D crystal); (b) computed absorption intensities of stretching and deformation bands, as function of the expansion factor f; the red lines indicate the intensity values predicted for the isolated chain; values of the computed absorption intensities, normalized to one CH oscillator, are reported in Table IV.

the isolated chain, while deformation intensity decays very quickly in the first steps of expansion (it halves in between the first and the second step). This behaviour indicates that the overall intensity increase due to the polarization of the bulk in the 3D crystal is a long range effect, while the additional mechanism responsible of the selective and remarkable intensity enhancement of deformation modes is related to the close packing between first neighbouring chains.

C. Comparison with oligomers: Single chain model vs all-trans n-alkanes *in vacuo*

In order to discuss the relationships between absorption intensities of an all-trans infinite PE chain and those of its oligomers, *in vacuo*, we compare here the IR spectrum for the 1D crystal with the spectra predicted for several n-alkanes of different lengths in their all-trans conformation. For a better comparison, following a computational procedure firstly proposed in Ref. 63, we decided to remove the contribution of the methyl end groups by introducing fictitious masses on their hydrogen atoms, to decouple methyl vibrations from CH_2 modes (see in supplementary material data obtained from calculations on chains carrying "real" masses also for methyl hydrogen atoms).

From Figure 4, we can realize that even the shorter chain ($C_{14}H_{30}$) shows a spectral pattern similar to that of the 1D PE crystal: the main bands possess the same frequencies and their intensities (Table V)—normalized to the number of CH bonds—are very close in value.

Minor features appear in the region below 1600 cm^{-1}, where the n-alkanes spectra show a multiplicity of weak bands, absent in the case of 1D crystal. These bands corresponds to the well-known rocking, scissoring, and wagging sequences, namely, to normal vibrations corresponding to $q \neq 0$ phonons of the infinite chain, which are inactive for symmetry reasons in the IR spectrum of the 1D crystal.[11–15] As expected, sequences of bands associated to $q \neq 0$ transitions weaken when the chain length grows, approaching the infinite chain limit. The results obtained demonstrate that the IR pattern (frequencies and intensities) predicted for the infinite single chain model is fully consistent with predictions for isolated n-alkanes, without PBC, thus indicating that the oligomer approach holds also from the viewpoint of the DFT predictions.

TABLE V. Calculated (B3LYP/6-31G(d,p)) intensity values for the relevant spectral regions (values are normalized to the number of CH bonds in the polymethylene chains of PE (single chain) and of some selected n-alkanes (isolated molecules, all trans conformation). In the cases of oligomers, the contributions of the methyl groups are removed by adopting fictitious heavy masses for methyl hydrogen atoms (see text).

	$I^{stretching}$/CH (km/mol)	$I^{deformation}$/CH (km/mol)	$R = I^{stretching}/I^{deformation}$
3D crystal	75	5.26	14
1D crystal	32	0.7	55
$C_{50}H_{102}$ (weighted ends)	32	0.8	40
$C_{30}H_{62}$ (weighted ends)	32	0.9	37
$C_{14}H_{30}$ (weighted ends)	33	1.1	30

D. Intermolecular effects: Bundle of chains vs 3D crystal

The extent of the chain-chain interaction in the 3D packing can be investigated considering, instead of an ideally infinite assembly of chains (3D crystal), a bundle of chains characterized by the typical packing of the orthorhombic crystal of PE. By means of this model, it should be possible to clearly disentangle effects on the spectrum due to short range intermolecular interactions from the polarization effects related to the simulation of a chain molecule embedded in an ideally infinite 3D crystal, described by means of PBC. Moreover, long range vs first neighbour interactions will be discussed by comparing the results obtained for bundles of

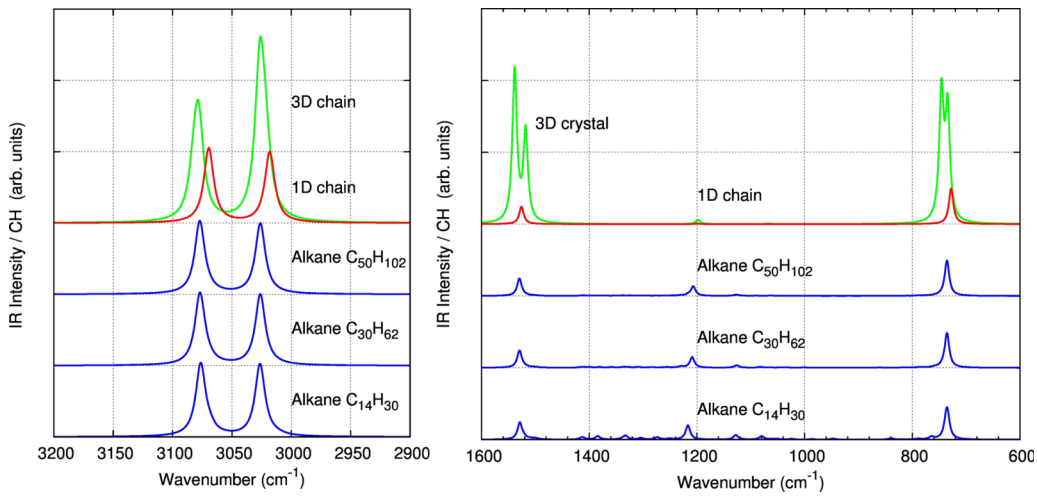

FIG. 4. Comparison among the computed (B3LYP/6-31G(d,p)) IR spectra of PE (single chain) and the spectra of some selected n-alkanes (isolated molecules, all trans conformation). In the case of oligomers, the contributions of the methyl groups are removed by adopting fictitious heavy masses for methyl hydrogen atoms (see text). Intensity values are reported in Table VI, for the relevant spectral regions (values are normalized to the number of CH bonds in the polymethylene chains).

different sizes. Calculations have been carried out according to the following models:

i. *Cluster 1*: A bundle of 1D chains where the inner chain should experience interactions like those arising from the interactions with first neighbour chains in the crystal. The model is a 1D crystal made by a central PE chain surrounded by six chains arranged according to the geometry of the 3D orthorhombic crystal. PBC along the chain axis direction are managed in the framework of the CRYSTAL code. The masses of the atoms belonging to chains in the external shell have been arbitrarily replaced with heavy masses, in order to avoid the vibrational coupling with the central chain. By this way, we aimed at describing the bare effect of intermolecular interactions among first-neighbour chains on the intensities of the vibrational modes localized on one individual chain.
ii. *Cluster 2*: The model is similar to that described at point 1, but in this case, a more sizeable cluster is considered; namely, the inner chain is surrounded by two subsequent shells of chains, the first one formed by 6 chains and the second one by 12 chains. Also in this case, the geometry of the 3D crystal is adopted and all the chains around the central one carry fictitious heavy masses.

Cluster 1 model has been also applied to finite length chains ($C_{14}H_{30}$) in order to underline possible differences while passing from an infinite bundle to a bundle of chains of finite length.

Both clusters 1 and 2 have been built starting from the optimized geometry of the 3D crystal, and then relaxing the geometry. Only small changes in the internal coordinates have been obtained. The results are reported in Figure 5 and are quite interesting.

First of all, it is apparent that the introduction of the second shell (Cluster 2) does not modify the results obtained with Cluster 1 model, thus suggesting that the relevant interactions are confined to first neighbour chains, as expected in the case of relatively weak van der Waals interactions.

While comparing the predictions for the polymer clusters with those for 3D crystal and 1D crystal of PE—see Table VI—we can make the following observations:

a. Rocking and scissoring splitting is not reproduced by the clusters models, because the vibrational coupling among adjacent chains is removed thanks to the introduction of "heavy masses."
b. The frequencies of the two main CH stretching bands in the spectra of the clusters result to be blue shifted if compared to those of the isolated chain. As already mentioned, a thermally induced shift of the CH stretching features toward lower wavenumbers has been experimentally observed[56] in the case of PE. Interestingly, this effect is present even if the peripheral chains in the two clusters carry fictitious heavy masses, showing that the predicted blue-shift is not a mere consequence of the vibrational coupling between chains but it is induced by the crystal field, through first-neighbor interactions.
c. The intensity ratio between d+ and d− bands in the clusters is close to that predicted for the 1D crystal. This confirms that the mixing of d+ and d− in the phonon eigenvectors of the 3D crystal is responsible of the—apparently spurious—overestimation of d+ band.
d. The ratio between absorption intensities in the 3D crystal and in the thickest bundle (Cluster-1D, 2 shells) is in the range 2.61–2.62, very close to the factor $F = 2.72$ estimated in Section IV A, based on geometrical and classical electrostatics considerations. Based on previous experience,[54] very large clusters are needed in order to achieve numerical agreement on these factors.
e. The cluster models allow to obtain the same intensity ratio between the stretching and the deformation regions

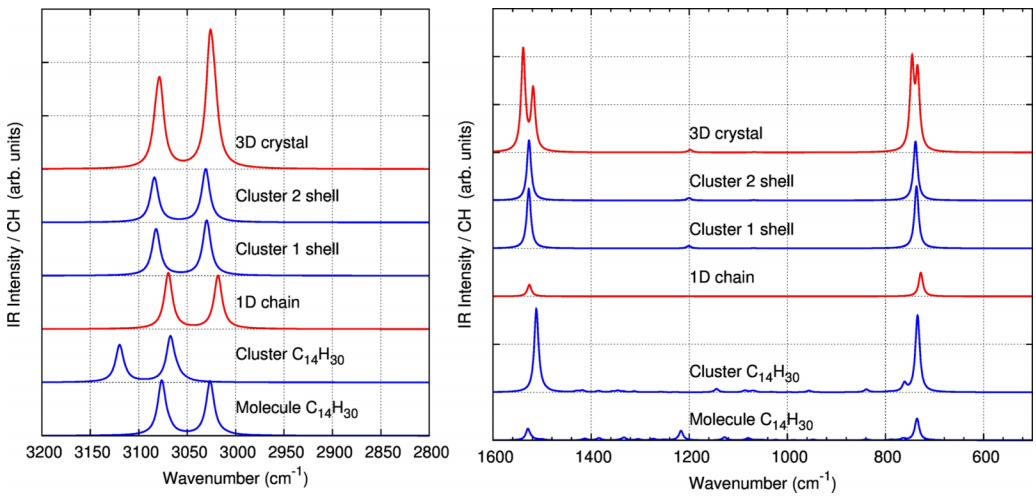

FIG. 5. Comparison among the computed IR spectra of PE (3D crystal, B3LYP-D2/6-31G(d,p) calculation and 1D crystal, B3LYP/6-31G(d,p) calculation) and the spectra of bundles of PE chains, described as 1D crystals (see text for the description of the clusters geometries, B3LYP-D2/6-31G(d,p) calculations). For the clusters, the contributions to the spectrum of the chains surrounding the central one is removed adopting fictitious heavy masses (see text). The two spectra at the bottom of the panel are obtained for $C_{14}H_{30}$ *in vacuo* (B3LYP/6-31G(d,p) calculation) and for a cluster (B3LYP-D2/6-31G(d,p) calculation) of seven $C_{14}H_{30}$ molecules. Also in this case, heavy masses have been adopted in order to decouple vibrations of the methyl groups and of the peripheral chains.

TABLE VI. Computed (B3LYP-D2/6-31G(d,p)) intensity values, for the relevant spectral regions (values are normalized to the number of CH bonds in the polymethylene chains). In parentheses, intensity data obtained from calculations on clusters, where all chains carry "real" masses. Intensity data from calculations carried out for a cluster of seven $C_{14}H_{30}$ molecules are also reported and compared with calculations on the molecule *in vacuo*.

	$I^{stretching}$/CH (km/mol)	$I^{deformation}$/CH (km/mol)	$R = I^{stretching}/I^{deformation}$
3D crystal	75	5.26	14
Cluster (1D crystal; 2 shells)	28.74 (29.75)	1.995 (1.73)	14.40 (17.16)
Cluster (1D crystal; 1 shell)	29.84 (30.52)	2.04 (1.59)	14.66 (19.23)
1D crystal (isolated chain)	32	0.58	55
Cluster of molecules ($C_{14}H_{30}$—1 shell, weighted ends)	26 (29.97)	3.2 (3.18)	8.13 (9.43)
$C_{14}H_{30}$ (isolated molecule; weighted ends)	33 (33.61)	1.1 (1.92)	30 (17.50)
PE, experimental	...	...	9.3

predicted by the calculation for the 3D crystal, in agreement with the experimental observation.

f. On the other hand, if we directly compare the intensity values obtained for the clusters with the intensities of the isolated chain (Figure 5) we can observe that the bending region is 3-4 times stronger in the cluster case. This factor is comparable with the factor 3 measured by Snyder[43] following solid-gas transition for several n-alkanes and clearly demonstrates that short range intermolecular interactions are responsible for an effective packing of first neighbouring chains. In this case, the inter-chain distance is shorter enough to give rise to non-negligible electro-optical interactions, which in turns determine the observed enhancement of the bending intensities in solid phase.

g. On the opposite, the intensity of the CH-stretching region predicted for the cluster models shows negligible differences with respect to that of the isolated chain. Also this fact finds a nice correspondence with the available experimental data, showing that CH stretching intensities are scarcely affected by heating.

The results obtained for the isolated $C_{14}H_{30}$ chain and for its cluster (Gaussian09 calculations) parallels all the finding commented above for the PE case.

In Table VI, the average intensity values taken from calculations on the same clusters keeping "real" masses for all the chains (molecules) are also reported, showing that the observations on the intensity trends reported above still hold independently from the vibrational coupling between adjacent chains.

E. Oligomers in the crystalline phase: Hexane

The phenomena induced in the IR spectrum of PE by intermolecular interactions occurring in the crystal are common to its oligomers, as widely demonstrated by several papers where a joint analysis of the spectrum of PE and of its oligomers is presented.[19–21,43–45]

In the following, we will show that the trends predicted adopting different models of PE (single chain, cluster of chains, and 3D crystal) can be found also for short n-alkanes. Since the calculation of the spectrum of the 3D crystal is computationally demanding in the case of oligomers, we decided to focus on the case of hexane.

The intensity data relevant for the discussion are reported in Figure 6 and Table VII, showing trends similar to those found in the case of PE. In particular, the intensity of the

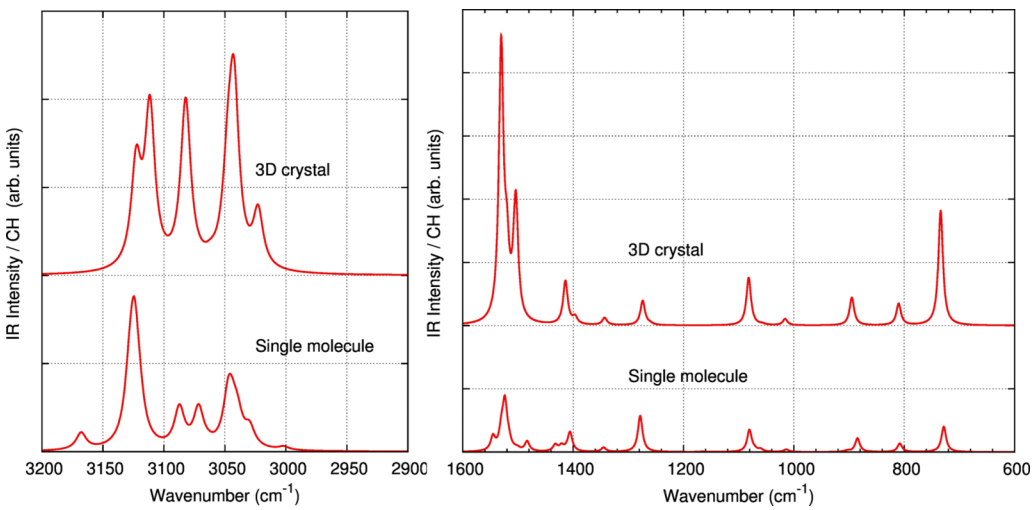

FIG. 6. Comparison among the computed IR spectra of hexane in the 3D crystal (B3LYP-D2/6-31G(d,p) calculation) and for the isolated molecule (B3LYP/6-31G(d,p) calculation), in all-trans conformation. Computed average intensity values are reported in Table VII.

TABLE VII. Computed (B3LYP-D2/6-31G(d,p)) average intensity values of hexane in the 3D crystal and for the isolated molecule (B3LYP/6-31G(d,p) calculation), in all-trans conformation, in the relevant spectral regions (values are normalized to the number of CH bonds). In parentheses, the experimental intensity data (from Ref. 47) are reported.

	$I^{stretching}$/CH (km/mol)	$I^{deformation}$/CH (km/mol)	$R = I^{stretching}/I^{deformation}$
3D - crystal	65.56	9.47	6.93
Isolated molecule	34.97	3.64	11.41
Experimental	34	5.01	6.80

stretching region halves from the case of the 3D crystal to that of the isolated molecule. Moreover, the deformation intensities markedly decrease—by a factor of 4.3—from 3D crystal to the molecule.

The comparison with the absolute absorption intensity values experimentally observed (Table VII) gives a further support to the conclusions drawn for the case of PE. In particular, an intrinsic increase of the deformation intensity—led by intermolecular packing—is predicted. Indeed, the intensity ratio between stretching and deformation region predicted for the hexane crystal (R = 6.93) is in very nice agreement with the experimental value (R = 6.80).

V. SUMMARY AND CONCLUSIONS

This work aims to assess the description of the IR spectra of polymers in the crystalline state as obtained through DFT calculations, carried out by means of CRYSTAL14 code.

The analysis has been performed according to three different models, adopted for the description of PE, namely:

(a) The all trans isolated chain, described as a 1D crystal;
(b) The 3D crystal characterized by an orthorhombic cell and two PE chains in the unit cell;
(c) Two different clusters, mimicking the intermolecular environment in the crystal, without explicit application of periodic boundary condition in the **ab** plane, orthogonal to the chain axis **c**.

Moreover, several oligomers have been considered for sake of comparison, namely:

(i) Isolated n-alkanes in all-trans conformation ($C_{50}H_{102}$, $C_{30}H_{62}$, $C_{14}H_{30}$), in order to assess the coherence of the oligomer approach with the description of the vibrations of an isolated polymer chain, modelled as an infinite 1D crystal.
(ii) A cluster of $C_{14}H_{30}$ chains to assess the effect of PBC in the **c** axis direction in presence of intermolecular interaction mimicking the real molecular environment in the crystal.
(iii) The 3D crystal of hexane and the isolated molecule in trans conformation in order to verify whether the conclusion drawn for the case of PE has a counterpart in the case of a small n-alkane.

The analysis of the results obtained has been carried out through the comparison with the available experimental data, that is,

- IR spectra of highly crystalline PE and of solid crystalline n-alkanes.
- Thermal evolution of the IR intensities (from low temperature solid state to gas phase in the case of n-alkanes; from low temperature solid state to the melt for PE).

The main conclusions can be summarized as follows:

1. PBC in the direction of the chain axis give spectra fully compatible with the modelling of finite size oligomers. This fact tells us that the oligomer approach, proposed in pioneering works dealing with the interpretation and modelling of polymer spectra, is perfectly suitable also in the light of a first principle approach.
2. Intermolecular interactions occurring when chains are packed in the crystal are far from being negligible for a good prediction of the spectra of the solid crystalline phase. Calculations carried out on 3D PE crystal allow to predict the observed crystal splitting of rocking and scissoring bands and demonstrate that the effect of chains packing induces a remarkable variation of the intrinsic deformation intensities. The phenomenon was observed in the past by Snyder,[43,44] who ascribed the intensity decrease with heating to the coupling of the rocking and scissoring vibrations with large amplitude torsional motions, thermally activated. The results obtained, through models which do not take explicitly into account thermal excitations and/or an-harmonic couplings, cast new light on the role of electro-optical intermolecular interactions between first neighboring closely packed molecules.
3. The absolute values of absorption intensities predicted for 3D crystals (PE and hexane) show an overall enhancement by a factor of about two, as shown by a careful discussion of the predictions obtained for the CH stretching region. The different computational setup exploited in this work gives similar results, which can be fully rationalized considering the effect of the local field and the difference between refractive index of the material and the vacuum.
4. Point 3 above suggests that the comparison between spectroscopic quantities (i.e., IR and Raman intensities) predicted for an isolated unit and for a unit belonging to a crystal requires some precaution. The conversion factor needed varies according to the dimensionality of such units (0D—molecule; 1D—polymer; 2D—slab).

SUPPLEMENTARY MATERIAL

See supplementary material for additional tables and figures about the comparison of experimental and DFT computed spectroscopic data.

ACKNOWLEDGMENTS

The authors would like to thank Bartolomeo Civalleri for useful discussions and suggestions.

[1]Y. Hu, P. C. Painter, and M. M. Coleman, Macromol. Chem. Phys. **201**, 470 (2000).
[2]J. S. Stephens, D. B. Chase, and J. F. Rabolt, Macromolecules **37**, 877 (2004).

[3]G. Pimentel and A. McClellan, *The Hydrogen Bond* (W. H. Freeman and Company, 1960).
[4]C. Quarti, A. Milani, B. Civalleri, R. Orlando, and C. Castiglioni, J. Phys. Chem. B **116**, 8299 (2012).
[5]A. Milani, J. Phys. Chem. B **119**, 3868 (2015).
[6]D. Galimberti, C. Quarti, A. Milani, L. Brambilla, B. Civalleri, and C. Castiglioni, Vib. Spectrosc. **66**, 83 (2013).
[7]A. Milani, J. Zanetti, C. Castiglioni, E. Di Dedda, S. Radice, G. Canil, and C. Tonelli, Eur. Polym. J. **48**, 391 (2012).
[8]A. Milani, C. Castiglioni, E. Di Dedda, S. Radice, G. Canil, A. Di Meo, R. Picozzi, and C. Tonelli, Polymer **51**, 2597 (2010).
[9]F. Muniz-Miranda, M. Pagliai, G. Cardini, and R. Righini, J. Chem. Phys. **137**, 244501 (2012).
[10]S. Krimm, *Fortschritte Hochpolym.-Forsch* (Springer Berlin Heidelberg, 1960), pp. 51–172.
[11]G. Zerbi, Appl. Spectrosc. Rev. **2**, 193 (1969).
[12]G. Zerbi, A. J. Barnes, and W. J. Orville-Thomas, Vib. Spectrosc. Trends Ch. 24, p. 379 (1977).
[13]G. Zerbi, Adv. Infrared Raman Spectrosc. **11**, 301 (1984).
[14]C. Castiglioni, *Handbook of Vibrational Spectroscopy* (John Wiley & Sons, Ltd., 2006).
[15]B. Bunsenges, Für Phys. Chem. **86**, 960 (1982).
[16]A. Milani and D. Galimberti, Macromolecules **47**, 1046 (2014).
[17]A. Milani, C. Castiglioni, and S. Radice, J. Phys. Chem. B **119**, 4888 (2015).
[18]D. Galimberti and A. Milani, J. Phys. Chem. B **118**, 1954 (2014).
[19]R. G. Snyder and J. H. Schachtschneider, Spectrochim. Acta **19**, 85 (1963).
[20]J. H. Schachtschneider and R. G. Snyder, Spectrochim. Acta **19**, 117 (1963).
[21]R. G. Synder and J. H. Schachtschneider, Spectrochim. Acta **21**, 169 (1965).
[22]R. Dovesi, V. R. Saunders, C. Roetti, R. Orlando, C. M. Zicovich-Wilson, F. Pascale, B. Civalleri, K. Doll, N. M. Harrison, I. J. Bush, P. D'Arco, M. Llunell, M. Causà, and Y. Noel, *CRYSTAL14 User's Manual* (University of Torino, Torino, 2014).
[23]R. Dovesi, R. Orlando, A. Erba, C. M. Zicovich-Wilson, B. Civalleri, S. Casassa, L. Maschio, M. Ferrabone, M. De La Pierre, P. D'Arco, Y. Noël, M. Causà, M. Rérat, and B. Kirtman, Int. J. Quantum Chem. **114**, 1287 (2014).
[24]F. J. Torres, B. Civalleri, A. Meyer, P. Musto, A. R. Albunia, P. Rizzo, and G. Guerra, J. Phys. Chem. B **113**, 5059 (2009).
[25]F. J. Torres, B. Civalleri, C. Pisani, P. Musto, A. R. Albunia, and G. Guerra, J. Phys. Chem. B **111**, 6327 (2007).
[26]A. M. Ferrari, B. Civalleri, and R. Dovesi, J. Comput. Chem. **31**, 1777 (2010).
[27]C. Quarti, A. Milani, and C. Castiglioni, J. Phys. Chem. B **117**, 706 (2013).
[28]D. Braga, L. Chelazzi, F. Grepioni, L. Maschio, S. Nanna, and P. Taddei, Cryst. Growth Des. **16**, 2218 (2016).
[29]M. Tasumi and S. Krimm, J. Chem. Phys. **46**, 755 (1967).
[30]S. Krimm, C. Y. Liang, and G. B. B. M. Sutherland, J. Chem. Phys. **25**, 549 (1956).
[31]N. Karasawa, S. Dasgupta, and W. A. Goddard, J. Phys. Chem. **95**, 2260 (1991).
[32]J. Barnes and B. Fanconi, J. Phys. Chem. Ref. Data **7**, 1309 (1978).
[33]S. Abbate, M. Gussoni, G. Masetti, and G. Zerbi, J. Chem. Phys. **67**, 1519 (1977).
[34]E. Koglin and R. J. Meier, Comput. Theor. Polym. Sci. **9**, 327 (1999).
[35]R. J. Meier, Polymer **43**, 517 (2002).
[36]A. Tarazona, E. Koglin, B. B. Coussens, and R. J. Meier, Vib. Spectrosc. **14**, 159 (1997).
[37]S. Abbate, G. Zerbi, and S. L. Wunder, J. Phys. Chem. **86**, 3140 (1982).
[38]R. A. MacPhail, H. L. Strauss, R. G. Snyder, and C. A. Elliger, J. Phys. Chem. **88**, 334 (1984).
[39]R. G. Snyder, J. Mol. Spectrosc. **7**, 116 (1961).
[40]G. Zerbi, R. Magni, M. Gussoni, K. H. Moritz, A. Bigotto, and S. Dirlikov, J. Chem. Phys. **75**, 3175 (1981).
[41]C. Castiglioni, M. Gussoni, and G. Zerbi, J. Chem. Phys. **95**, 7144 (1991).
[42]M. Gussoni, S. Abbate, and G. Zerbi, J. Chem. Phys. **71**, 3428 (1979).
[43]R. G. Snyder, M. Maroncelli, H. L. Strauss, and V. M. Hallmark, J. Phys. Chem. **90**, 5623 (1986).
[44]H. Hagemann, R. G. Snyder, A. J. Peacock, and L. Mandelkern, Macromolecules **22**, 3600 (1989).
[45]H. L. Casal, D. G. Cameron, and H. H. Mantsch, Can. J. Chem. **61**, 1736 (1983).
[46]S. Abbate, M. Gussoni, and G. Zerbi, J. Chem. Phys. **70**, 3577 (1979).
[47]R. G. Snyder, J. Chem. Phys. **42**, 1744 (1965).
[48]M. J. Frisch, G. W. Trucks, J. R. Cheeseman, G. Scalmani, M. Caricato, H. P. Hratchian, X. Li, V. Barone, J. Bloino, G. Zheng, T. Vreven, J. A. Montgomery, G. A. Petersson, G. E. Scuseria, H. B. Schlegel, H. Nakatsuji, A. F. Izmaylov, R. L. Martin, J. L. Sonnenberg, J. E. Peralta, J. J. Heyd, E. Brothers, F. Ogliaro, M. Bearpark, M. A. Robb, B. Mennucci, K. N. Kudin, V. N. Staroverov, R. Kobayashi, J. Normand, A. Rendell, R. Gomperts, V. G. Zakrzewski, M. Hada, M. Ehara, K. Toyota, R. Fukuda, J. Hasegawa, M. Ishida, T. Nakajima, Y. Honda, O. Kitao, and H. Nakai, GAUSSIAN 09, Gaussian, Inc., 2009.
[49]A. Becke, J. Chem. Phys. **98**, 5648 (1993).
[50]C. Lee, W. Yang, and R. Parr, Phys. Rev. B **37**, 785 (1988).
[51]S. Grimme, J. Comput. Chem. **25**, 1463 (2004).
[52]S. Grimme, J. Comput. Chem. **27**, 1787 (2006).
[53]B. Civalleri, C. M. Zicovich-Wilson, L. Valenzano, and P. Ugliengo, CrystEngComm **10**, 405 (2008).
[54]L. Maschio, B. Kirtman, R. Orlando, and M. Rèrat, J. Chem. Phys. **137**, 204113 (2012).
[55]C. W. Bunn, Trans. Faraday Soc. **35**, 482 (1939).
[56]I.-E. Mavrantza, D. Prentzas, V. G. Mavrantzas, and C. Galiotis, J. Chem. Phys. **115**, 3937 (2001).
[57]N. Bloembergen, *Nonlinear Optics* (Benjamin, 1965).
[58]J. Zyss and J. L. Oudar, Phys. Rev. A **26**, 2028 (1982).
[59]B. Szigeti, Trans. Faraday Soc. **45**, 155 (1949).
[60]M. Ferrero, M. Rérat, B. Kirtman, and R. Dovesi, J. Chem. Phys. **129**, 244110 (2008).
[61]S. Salustro, L. Maschio, B. Kirtman, M. Rérat, and R. Dovesi, J. Phys. Chem. C **120**, 6756 (2016).
[62]R. Kishi, S. Bonness, K. Yoneda, H. Takahashi, M. Nakano, E. Botek, B. Champagne, T. Kubo, K. Kamada, K. Ohta, and T. Tsuneda, J. Chem. Phys. **132**, 094107 (2010).
[63]N. B. da Costa, A. J. A. Aquino, M. N. Ramos, C. Castiglioni, and G. Zerbi, J. Mol. Struct.: THEOCHEM **305**, 19 (1994).